Scheme III
Further Thermal Reactions among Pyrolysis Products

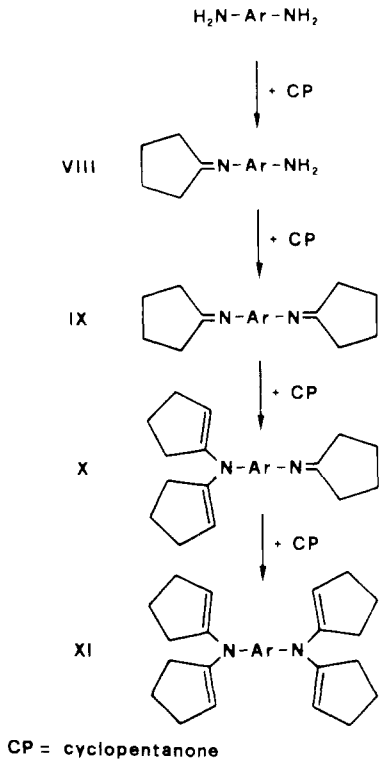

3, CO_2 is observed. It is likely that it originates from the pyrolysis of isocyanates (Scheme IIb), which are detected intact by DPMS (Table III), whereas they may undergo further degradation in the Py–GCMS experiments.

In the case of polymer V, the primary thermal decomposition mechanism is analogous to that of polymers III and IV. In fact, compounds similar to those observed for polymers III and IV are formed (Table IV). *N*-Methyl substitution should prevent the occurrence of the reaction shown in Scheme IIb, but small amounts of cyclopentanone are nevertheless present among the pyrolysis products (Figure 8 and Table IV). It therefore may be hypothesized that cyclopentanone is formed from carboxylic acid end groups, as already proposed by Wiloth.[17]

Acknowledgment. Partial financial support from the Italian Ministry of Public Education and from Consiglio Nazionale delle Ricerche (Roma), Finalized Project of Fine and Secondary Chemistry, is gratefully acknowledged.

Registry No. I (copolymer), 55425-95-1; I (SRU), 55445-71-1; II (copolymer), 55426-01-2; II (SRU), 55445-65-3; III (copolymer), 31451-66-8; III (SRU), 25949-52-4; IV (copolymer), 86924-58-5; IV (SRU), 52216-11-2; V (copolymer), 86893-64-3; V (SRU), 86893-41-6; VII, 76304-78-4; *m*-$H_2NC_6H_4NH_2$, 108-45-2; 4,4′-$H_2NC_6H_4CH_2C_6H_4NH_2$, 101-77-9; succinic anhydride, 108-30-5; cyclopentanone, 120-92-3.

References and Notes

(1) Foti, S.; Montaudo, G. In *Analysis of Polymer Systems*; Bark, L. S., Allen, N. S., Eds.; Applied Science: London, 1982; p 103.
(2) Schulten, H. R.; Lattimer, R. P. *Mass Spectrom. Rev.*, **1984**, *3*, 231.
(3) Montaudo, G.; Puglisi, C. In *Developments in Polymer Degradation*; Grassie, N., Ed.; Applied Science: London, 1986; Vol. 7.
(4) (a) Foti, S.; Giuffrida, M.; Maravigna, P.; Montaudo, G. *J. Polym. Sci., Polym. Chem. Ed.* **1983**, *21*, 1567, 1583, 1599. (b) *Ibid.* **1984**, *22*, 1201, 1217. (c) *Ibid.* **1985**, *23*, 1145, 1731.
(5) Ballistreri, A.; Garozzo, D.; Giuffrida, M.; Maravigna, P.; Montaudo, G. *J. Polym. Sci., Polym. Chem. Ed.* **1986**, *24*, 331.
(6) Garozzo, D.; Giuffrida, M.; Montaudo, G. *Macromolecules* **1986**, *19*, 1643.
(7) Bhuiyan, A. L. *Polymer* **1984**, *25*, 1699.
(8) Schulten, H. R.; Dussel, H. J. *J. Anal. Appl. Pyrolysis* **1980/1981**, *2*, 293.
(9) Khanna, Y. P.; Pearce, E. M.; Smith, J. S.; Burkitt, D. T.; Njuguna, H.; Hindenlang, D. M.; Forman, B. D. *J. Polym. Sci., Polym. Chem. Ed.* **1981**, *19*, 2817.
(10) Brown, J. R.; Power, A. J. *Polym. Degrad. Stab.* **1982**, *4*, 379, 479.
(11) Ohtani, H.; Nagaya, T.; Sugimura, Y.; Tsuge, S. *J. Anal. Appl. Pyrolysis* **1982**, *4*, 117.
(12) Conway, D. C.; Marak, R. *J. Polym. Sci., Polym. Chem. Ed.* **1982**, *20*, 1765.
(13) Karydas, A. C.; Kapuscinska, M.; Pearce, E. M. *Eur. Polym. J.* **1983**, *19*, 935.
(14) Bahr, U.; Lüderwald, I.; Muller, R.; Schulten, H. R. *Angew. Makromol. Chem.* **1984**, *120*, 163.
(15) Bletsos, I. V.; Hercules, D. M.; Greifendorf, D.; Benninghoven, A. *Anal. Chem.* **1985**, *57*, 2384.
(16) Wiloth, F.; Schindler, E. *Chem. Ber.* **1967**, *100*, 2373.
(17) Wiloth, F. *Makromol. Chem.* **1971**, *144*, 283.
(18) Reinisch, G.; Gohlke, U.; Ulrich, H. H. *Makromol. Chem., Suppl.* **1979**, *3*, 177.
(19) Garozzo, D.; Giuffrida, M.; Montaudo, G., to be published.
(20) Ballistreri, A.; Foti, S.; Montaudo, G.; Pappalardo, S.; Scamporrino, E. *J. Polym. Sci., Polym. Chem. Ed.* **1979**, *17*, 2469.

On the Structure of the Quenched Mesomorphic Phase of Isotactic Polypropylene

P. Corradini,* V. Petraccone, C. De Rosa, and G. Guerra

Dipartimento di Chimica, Università di Napoli, 80134 Napoli, Italy. *Received May 13, 1986*

ABSTRACT: The measured wide-angle X-ray diffraction intensity of the quenched mesomorphic phase of isotactic polypropylene is compared with the Fourier transforms of various models of chain aggregates. The calculations were performed on small bundles of threefold helices packed as in the hexagonal (β) and monoclinic (α) forms and on more disordered models showing both hexagonal and monoclinic features. Our results indicate that, in addition to the local parallelism of chains, a fairly high correlation of distances must be present within each chain and between neighboring chains in mesomorphic polypropylene. The local correlations between chains are probably nearer to those characterizing the crystal structure of the monoclinic form than to those characterizing the structure of the hexagonal form.

Introduction

The occurrence of a partially ordered phase (mesomorphic phase) together with an amorphous phase in rapidly quenched samples of isotactic polypropylene (i-PP) was pointed out many years ago.[1-3] On the basis of X-ray diffraction patterns and IR spectra it was recognized[1,2] that in the partially ordered phase of i-PP the individual chains maintain the threefold helical conformation and the chains

0024-9297/86/2219-2699$01.50/0

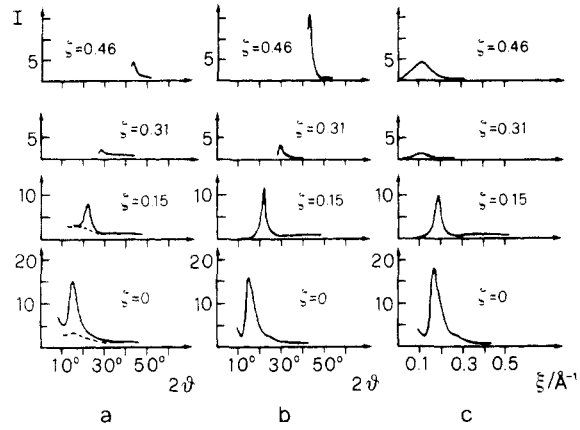

Figure 1. Experimental X-ray diffraction patterns of a stretched film of mesomorphic isotactic polypropylene at the indicated reciprocal lattice coordinate ζ (Å^{-1}) (full lines): (a) measured intensities as a function of 2θ, (in dashed lines, the amorphous halo, measured at ζ = 0.08 Å^{-1}); (b) corrected intensities as a function of 2θ; (c) corrected intensities as a function of the reciprocal lattice coordinate ξ.

are parallel. It was also recognized that the packing of the chains perpendicularly to their axes is more disordered than along the axes, though the relative displacements and orientations of neighboring chains do not appear to be completely random. For this reason, Natta, Peraldo, and Corradini[1] gave the name "smectic" to this mesophase, thus indicating a degree of order higher than that of an ideal nematic liquid crystalline phase, in which the only degree of order is the molecular parallelism.

The presence of some correlation between the positions of adjacent helices, their z coordinates, and their rotational coordinates was also suggested by Wyckoff.[3]

An even higher degree of order was proposed by Gailey and Ralston,[4] who suggested that the quenched material is composed of very small (50–100 Å) hexagonal crystals. This suggestion was simply based on the observation that the positions of the two most intense diffraction maxima of the partially ordered phase ($1/d$ = 0.17 Å^{-1}, $1/d$ = 0.24 Å^{-1}) are nearly coincident with the two most intense peaks of the hexagonal (β) crystalline form ($1/d$ = 0.18 Å^{-1}, $1/d$ = 0.24 Å^{-1}).[5]

Bodor et al.[6] assumed that the quenched form is composed of microcrystals of monoclinic polypropylene and concluded that crystal size broadening is responsible for the typical X-ray diffraction pattern. On the other hand, the rather diffuse X-ray diffraction pattern was associated by Miller[7] and subsequently by Zannetti et al.[8] with the occurrence of paracrystallinity (distortions of the monoclinic lattice of the second kind in the sense of Hosemann,[9] that is, with loss of long-range order).

Only a detailed model for the partially ordered phase of i-PP has been proposed.[10] However, this model has to be discarded[11] since nearly all the diffraction maxima were interpreted as equatorial reflections, in contrast with the X-ray patterns of the oriented quenched samples.

It is apparent that the structure of the partially ordered phase of i-PP obtained by quenching needs to be further clarified. To this end the Fourier transforms of various kinds of aggregates of helices will be compared in this paper with the measured diffraction intensities.[11]

Experimental Procedure and Method of Calculation

The X-ray diffraction patterns of stretched films of mesomorphic isotactic polypropylene are reported in Figure 1a. The layer lines were collected following the procedure described in ref 11, so that the intensities are

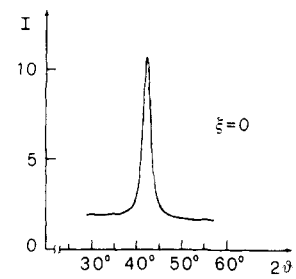

Figure 2. Diffraction intensity along the meridian (ξ = 0) collected for values of ζ around ζ = 0.461 Å^{-1} (third layer line) and reported as a function of 2θ.

reported as a function of the Bragg angle 2θ.

The amorphous halo, which was measured at ζ = 0.08 Å^{-1} as a function of 2θ, is reported in Figure 1a (dashed lines) and was subtracted from the intensities of the layer lines. The Lorentz–Polarization (LP) correction was then applied. (LP = $(1 + \cos^2 2\theta)/\sin 2\theta$ for all the layer lines according to the diffraction geometry.)

The intensities corrected in this way for the equator and for the three layer lines are reported in Figure 1b as a function of 2θ and in Figure 1c as a function of the reciprocal lattice coordinate ξ. The transformation of the corrected intensities $I(\theta)$ into $I(\xi)$ was performed graphically in such a way that

$$\int_{\xi_1(\theta_1)}^{\xi_2(\theta_2)} I(\xi)\, d\xi = K \int_{\theta_1}^{\theta_2} I(\theta)\, d\theta$$

for sufficiently small (θ_2–θ_1) intervals.

For the calculation of the Fourier transforms, we considered models with regular 3/1 helices of i-PP, packed with their axes strictly parallel.

The square of the modulus ($|F(\xi,\varphi,\zeta)|^2$) of the Fourier transform was calculated for each model as a function of the cylindrical reciprocal lattice coordinates ξ and ζ for a fixed value of the third coordinate φ. The mean value of $|F(\xi,\varphi,\zeta)|^2$ with respect to φ, henceforth indicated $\langle|F(\xi,\zeta)|^2\rangle$, was obtained by averaging the results for 90 different fixed rotations of the models around an axis parallel to the chain axes. The integral $I(\xi,\zeta) = \int_0^{2\pi}|F(\xi,\varphi,\zeta)|^2\, d\varphi$, which is the quantity to be compared with experimental data such as those of Figure 1c, is then obtained through multiplication of $\langle|F(\xi,\zeta)|^2\rangle$ by $2\pi\xi$.

Most of our calculations were performed without taking into account the further disorder of first and second order possibly present. To account for this kind of disorder, the calculated intensity may be multiplied by a "thermal factor" of the kind $\exp(-1/2 B_\xi \xi^2)\exp(-1/2 B_\zeta \zeta^2)$ in the approximation that the mean displacements of the atoms between themselves are independent of the distance. We have used both an isotropic parameter, $B_\xi = B_\zeta$ = 8 Å^2 (as used by Natta and Corradini in the solution of the crystalline structure of the α form of i-PP[2]), and anisotropic parameters, B_ξ = 20 Å^2 and B_ζ = 5 Å^2, on the more reasonable assumption that the disorder along the chain axis is less pronounced than in the lateral directions.

The diffracted intensity on the meridian for the third layer line (that is, the intensity at ξ = 0 for values of ζ around ζ = 0.46 Å^{-1}) is reported in Figure 2. The broadness along ζ of the diffraction indicates average coherent lengths of the helices along their axes of the order of 40 Å.

Our calculations of Fourier transforms were then performed on bundles of parallel chains, with axes having a length of 40 Å (20 monomeric units in a 3/1 conformation) and diameters of the aggregates of nearly 30 Å. This last value was indicated by the broadening of the reflections

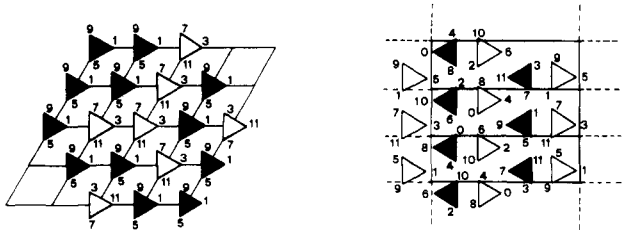

Figure 3. Representative limit models: (a) pseudohexagonal model with right- and left-handed helices generated at random in each site; (b) monoclinic model. The models are sketched as projections along the chain axis. The height of the methyl groups, which project on the vertices of the triangles, are expressed in twelfths of the c axis (c = 6.5 Å). The projection along the c axis of the trigonal (β) and monoclinic (α) unit cells are shown in (a) and (b), respectively. Clear and dark triangles refer to right- and left-handed chains, respectively.

on the equator and on the first layer line and is in agreement with the data of Wyckoff.[3] This does not exclude the possibility that the bundles may be larger, and even much larger, but any correlation about the relative position of the atoms is lost at distances of the order of magnitude indicated, according to the wide-angle X-ray diffraction data.

Results of the Calculations of Fourier Transforms

In the following we report only the results for some representative models among the many considered by us. We have considered first some limiting models corresponding to the two different hypotheses suggested by various authors that the X-ray diffraction spectrum of the mesomorphic form of i-PP may be interpreted as if it resulted from the diffraction of extremely small crystals, hexagonal (as observed for the β form[5]) or monoclinic (as observed for the α form[2]).

As far as the first hypothesis is concerned, we have considered two possibilities: (1) a model with isomorphous helices, for which the local structure may be described by a trigonal cell containing only one helix, as proposed for the β form of i-PP by Addink and Beintema,[12] and (2) pseudohexagonal models with the same equatorial projection of chains as in model 1, but with right- and left-handed chains generated at random in each site (Figure 3a). In these models, corresponding carbon atoms of the methyl groups were placed at the same height, as in model 1, for isomorphous helices while the carbon atoms of the methyl groups of enantiomorphic helices were displaced along the chain axes by $^1/_2c(\pm^4/_{12}c)$. This displacement is the one which diminishes as much as possible the calculated intensity at $\xi \simeq 0$ for the third layer line. An identical displacement was chosen by Turner-Jones[5] in order to optimize the contacts between enantiomorphic helices in a proposed model of the β structure.

As far as the second hypothesis is concerned (the α-structure), one of the calculated models is shown in Figure 3b).

The results of the calculations for the above reported models are shown in Figure 4 (full lines). For the pseudohexagonal models, differences in the calculated transforms arise from the various, randomly generated distributions of enantiomorphic helices (mainly on the third layer line). Therefore, we show in Figure 4a the mean value of the calculated intensity taken over a sufficiently representative number of random models.

Other models, of the kind shown in Figure 5, were built up of helices arranged according to the α or pseudohexagonal structure for different regions of the bundle: as an example, the model of Figure 5a contains a core with a pseudohexagonal arrangement of chains and two peripheral blocks with an α structure, while the model of Figure 5b contains a core having the α structure surrounded by helices in a pseudohexagonal arrangement. The results of the calculations for the above cited models are shown as full lines in parts a and b of Figure 6, respectively. Figure 6c reports instead the intensity of a hypothetical 30:70 mixture of the models of Figure 3a (pseudohexagonal structure) and Figure 3b (α structure).

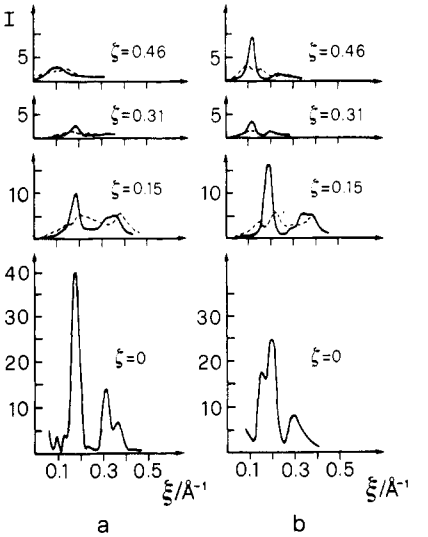

Figure 4. Representative results of the calculations of Fourier transforms on limiting pseudohexagonal and monoclinic models at the indicated ζ (Å^{-1}). Full lines: (a) average of the results for 10 models of the kind sketched in Figure 3a; (b) results for the model of Figure 3b. Dashed lines: calculated intensity after the introduction of random displacements in the relative height of neighboring chains.

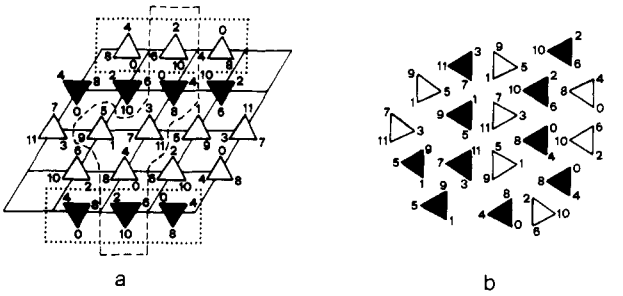

Figure 5. Typical models of chain bundles showing both pseudohexagonal and monoclinic features. (a) Model with a core of chains in a pseudohexagonal arrangement and two peripheral α blocks. (b) Model with a core having the α structure surrounded by chains in a pseudohexagonal arrangement. Clear and dark triangles refer to right- and left-handed chains, respectively.

All of the models considered have relative heights of neighboring chains strictly correlated. To look at the resulting differences in calculated intensities, we performed some calculations on similar models after the introduction of displacements in the relative height of neighboring chains. The resulting intensities are reported in Figures 4 and 6 as dashed or dotted lines.

Discussion and Conclusions

A comparison of the experimental diffraction data of Figure 1c with the results of the calculations of Fourier transforms, exemplified in Figures 4 and 6, allows us to make some considerations and conclusions as to the kind and extension of the order present in the mesomorphic quenched phase of i-PP.

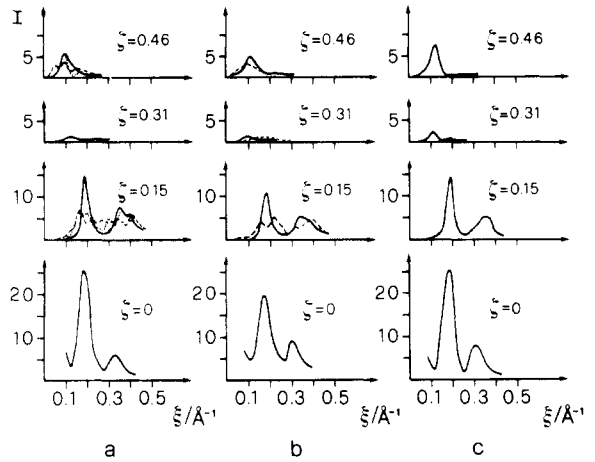

Figure 6. Representative results of the calculations of Fourier transforms on models of chain bundles showing both pseudohexagonal and monoclinic features at the indicated ζ (Å^{-1}). (a) Full line: results for the model of Figure 5a; dashed (dotted) line: results for the model of Figure 5a in which the height of the methyl groups of the chains enclosed in the dashed (dotted) line of Figure 5 is displaced $^6/_{12}c$ with respect to the indicated values. (b) Full line: results for the model of Figure 5b; dashed line: results for the model of Figure 5b after the introduction of random displacements in the relative height of neighboring chains. (c) Calculated intensity for a hypothetical 30:70 mixture of the models of Figure 3a (pseudohexagonal structure) and Figure 3b (monoclinic structure).

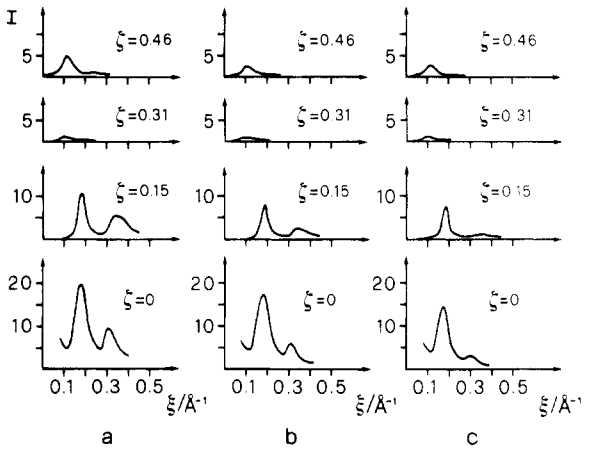

Figure 7. Calculated intensity for the model of Figure 5b at the indicated ζ (Å^{-1}), without the disorder factor (a) and multiplied by the disorder factor $\exp(-^1/_2B_\xi\xi^2)\exp(-^1/_2B_\zeta\zeta^2)$: (b) isotropic, $B_\xi = B_\zeta = 8$ Å^2; (c) anisotropic, $B_\xi = 20$ Å^2, $B_\zeta = 5$ Å^2.

First of all, the layering of the intensity diffracted from the quenched and subsequently drawn film gives a strong indication that in the partially ordered regions the macromolecular chains have conformations which are very nearly threefold helices (corresponding to a minimum of potential energy of the isolated chain[13]). Helix reversals are probably segregated at the termination of nearly straight chain segments having one helical sense.

The order of the atomic positions (and hence the correlation of interatomic distances) in the direction of the chain axes spans a longer range than in the perpendicular directions: as a result, the diffraction is better defined along the reciprocal lattice coordinate ζ than along ξ.

The position of the calculated intensity maxima is good for all the models on the zero and first layer lines and is good, though too sharp, for the second and third layer lines of the monoclinic model. In any case, the intensity distribution on the second and third layer lines is calculated at best for the more disordered models of Figure 6a,b and for the weighted sum of the intensities of pseudohexagonal and monoclinic models (Figure 6c).

The ratio of the intensity (I_0) of the peak at $\xi = 0.17$ Å^{-1} on the zero layer line to that of the peak at $\xi = 0.18$ Å^{-1} on the first layer line (I_1) is observed to be $I_0/I_1 = 2$. The calculated ratio for the hexagonal models (see, for example, Figure 4a) is 4 (as it was for the experimental diffraction pattern of the crystalline hexagonal modification of i-PP (β form)[5]) and becomes even higher for models in which neighboring helices lose correlation in relative heights (see, for example, Figure 4a, dashed line). Instead, the calculated I_0/I_1 ratio is in agreement with the observed ratio for the model having an α structure (Figure 4b) and for the models containing mixtures of monoclinic and pseudohexagonal structures, as in Figure 6.

Again for these models, if we withdraw the correlations in height between neighboring chains, the ratio I_0/I_1 becomes higher and then worse.

The bigger disagreements of the calculated intensities for completely α structures, as in Figure 4b, is the double-peak shape of the calculated intensity around $\xi = 0.17$ Å^{-1} for the zero layer line and the sharpness of the peak on the third layer line, features that are (partially) eliminated by introducing further disorder in the model (see Figre 6a,b). We obtained satisfactory agreement between calculated and observed intensities whenever we had a high proportion of nuclei containing at least 5–10 chains organized as in the monoclinic modification.

For all the models calculated without a "thermal factor", second-order peaks of low intensity are present on the zero and first layer lines for $\xi = 0.30$ Å^{-1} and $\xi = 0.34$ Å^{-1}, respectively. Figure 7 shows that the intensity of these second-order peaks may be strongly reduced by the application of such a factor. Good results are obtained with anisotropic parameters $B_\xi = 20$ Å^{-1} and $B_\zeta = 5$ Å^{-1} (Figure 7c).

From the calculations and considerations described, it is possible to draw some firm conclusions about the mesomorphic quenched form of i-PP. It is built up of bundles of chains, having conformations very nearly threefold helices and parallel among themselves. The helices are probably terminated at helix reversals and other conformational defects, the mean dimension of each segment of helix of one sense being of the order of 40 Å, as indicated by the width of the diffraction along ζ, around $\zeta = 0.46$ Å^{-1}, at $\xi = 0$. In our opinion, lateral order is not so well developed as conformational order, though the relative heights of the neighboring chains within each bundle are mainly correlated. The local correlations between chains are probably nearer to those characterizing the crystal structure of the monoclinic form than to those characterizing the structure of the hexagonal form.

In conclusion, in mesomorphic polypropylene short-range order is present within each chain and (to a lower degree) among chains. The chains are organized in bundles, for which any correlation about the relative position of the atoms is lost at distances of the order of 30–40 Å.

Since the structure cannot be described even locally by only one kind of unit cell with distortions of the second kind, the term paracrystalline could be used for its description if the term is intended to mean more or less distorted repetition in some directions (in our case, the chain axis) and probabilistic distributions of various arrangements (not reducible to one single kind of distorted unit cell) in other directions.

Acknowledgment. We acknowledge the financial support of the CNR and the Ministero della Pubblica Istruzione (Italy).

Registry No. i-PP, 25085-53-4.

References and Notes

(1) Natta, G.; Peraldo, M.; Corradini, P. *Rend. Accad. Naz. Lincei* **1959**, *26*, 14.
(2) Natta, G.; Corradini, P. *Nuovo Cimento, Suppl.* **1960**, *15*, 40.
(3) Wyckoff, H. W. *J. Polym. Sci.* **1962**, *62*, 83.
(4) Gailey, J. A.; Ralston, P. H. *SPE Trans.* **1964**, *4*, 29.
(5) Turner-Jones, A.; Aizlewood, J. M.; Beckett, D. R. *Makromol. Chem.* **1964**, *75*, 134.
(6) Bodor, G.; Grell, M.; Kallo, A. *Faserforsch. Textil-Tech.* **1964**, *15*, 527.
(7) Miller, R. L. *Polymer* **1960**, *1*, 135.
(8) Zannetti, R.; Celotti, G.; Armigliato, A. *Eur. Polym. J.* **1970**, *6*, 879.
(9) Hosemann, R. *Acta Crystallogr.* **1951**, *4*, 520.
(10) McAllister, P. B.; Carter, T. J.; Hinde, R. M. *J. Polym. Sci., Polym. Phys. Ed.* **1978**, *16*, 49.
(11) Guerra, G.; Petraccone, V.; De Rosa, C.; Corradini, P. *Makromol. Chem., Rapid Commun.* **1985**, *6*, 573.
(12) Addink, E. J.; Beintema, J. *Polymer* **1961**, *2*, 185.
(13) Corradini, P.; Petraccone, V.; Pirozzi, B. *Eur. Polym. J.* *1976*, *12*, 813.

^{13}C-Enriched End Groups of Polypropylene and Poly(1-butene) Prepared in the Presence of Bis(cyclopentadienyl)titanium Diphenyl and Methylalumoxane

Adolfo Zambelli,* Paolo Ammendola, Alfonso Grassi, Pasquale Longo, and Antonio Proto

Dipartimento di Fisica, Università di Salerno, 84100 Salerno, Italy. *Received May 20, 1986*

ABSTRACT: The stereochemical structure of ^{13}C-enriched end groups of isotactic polypropylene and poly(1-butene) prepared in the presence of bis(cyclopentadienyl)titanium diphenyl/methylalumoxane/^{13}C-enriched trialkylaluminum compounds is investigated by ^{13}C NMR analysis. The chain-end-controlled mechanism of isotactic-specific propagation is confirmed.

Propene and 1-butene have been polymerized at −60 °C in the presence of the homogeneous catalytic systems bis(cyclopentadienyl)titanium diphenyl/methylalumoxane/trimethylaluminum enriched with ^{13}C (CTP/MAO/TMA) and CTP/MAO/TEA (TEA = triethylaluminum enriched with ^{13}C on the methylene carbons). The polymers have been analyzed by ^{13}C NMR in order to check the mechanism of steric control and regiospecificity[1] by determining the stereochemical structure of the enriched end groups resulting from insertion of the monomers into the Mt–$^{13}CH_3$ or Mt$^{13}CH_2$–CH_3 bonds (Mt = metal atom of the catalytic complexes).

In a recent elegant paper, Ewen reported[2] that the above-quoted catalysts are partially isotactic specific and that the stereochemistry of the insertion of the monomer is controlled by the asymmetric configuration of the growing chain end (lk–1,3 asymmetric induction[2,3] replicating the configuration of the tertiary carbon of the growing chain end on the new asymmetric carbon resulting from the next insertion). The resonances of the natural-abundance carbons of polypropylene prepared in the presence of CTP/MAO/TMA (sample 1) and CTP/MAO/TEA (sample 2) (see Figure 1) are very similar to those already reported by Ewen,[2] and the analysis of the methyl stereochemical pentads[4] confirms that the stereochemical sequence of the propene units is in accord with the Bernoullian statistical model proposed by Bovey[5] with $P_{mP} = 0.8_8$ and $P_{rP} = 1 - P_{mP}$ (P_{mP} and P_{rP} are the probabilities of isotactic (m) and syndiotactic (r) placements of the propylene units[6] (see Table I)).

The additional resonances observed in the spectrum of sample 1 at 20.4_8, 20.7_6, 21.4_1, and 21.7_3 ppm from HMDS (hexamethyldisiloxane) and in the spectrum of sample 2 at 27.4_2, 27.7_2, 28.4_1, and 28.6_7 ppm from HMDS are due, respectively, to the ^{13}C-enriched methyls of the isobutyl end groups and to the ^{13}C-enriched methylenes of the 2-methylbutyl end groups. The splitting of the resonances is due to the possible diastereotopic positions of the enriched carbons with respect to the methyl substituents of the second and third inserted propylene units (see Figure 2).

Table I
Enantioselectivity of Propagation and Initiation Steps

sample	monomer	AlR_3	P_m[a]	$I_{\delta t}$[b]	$I_{\delta e}$[b]
1	propene	$Al(^{13}CH_3)_3$	0.8_7	0.5	0.5
2	propene	$Al(^{13}CH_2CH_3)_3$	0.8_8	0.7	0.3
3	1-butene	$Al(^{13}CH_3)_3$	0.6_0	0.3	0.7
4	1-butene	$Al(^{13}CH_2CH_3)_3$	0.6_0	≃0.5	≃0.5

[a] P_m corresponds to P_{mP} or P_{mB}, depending on the monomer (see text). [b] Probability of the indicated (δt or δe) placements evaluated from the relative areas of the resonances of the δt and δe enriched carbons ($I_{\delta t}$ = {[$\delta t\zeta t$] + [$\delta t\zeta e$]}/{[$\delta e\zeta e$] + [$\delta e\zeta t$] + [$\delta t\zeta t$] + [$\delta t\zeta e$]}.

The resonances under consideration have been assigned in previous papers[1] to the enriched carbons (either methyl or methylene) having the stereochemical locations[8] $\delta t\zeta t$, $\delta t\zeta e$, $\delta e\zeta t$, and $\delta e\zeta e$ at decreasing field (see Figure 2). The very presence of the resonances confirms, first of all, that the insertion of the monomer is primary (metal-to-C_1), at least for initiation and the two following propagation steps.[2] By considering the ratios between the areas of the resonances[10] of the enriched diastereotopic methyls of sample 1 ([$\delta t\zeta t$]:[$\delta e\zeta e$]:[$\delta t\zeta e$]:[$\delta e\zeta t$] = 1.0:1.0:0.15:0.15), one can visualize that insertion of propene on the Mt–$^{13}CH_3$ bond (initiation step) is not stereospecific. As discussed in ref 1, this conclusion comes from the fact that [$\delta e\zeta e$] = [$\delta t\zeta t$] and [$\delta t\zeta e$] = [$\delta e\zeta t$].

The fact that [$\delta e\zeta e$]/[$\delta e\zeta t$] = 6.7 shows that the insertion into the Mt–$CH_2CH(CH_3)CH_2CH(CH_3)$–$^{13}CH_3$ bond (second propagation step) is isotactic specific almost to the same extent as the following propagation steps. In fact (see Table I), it is also $P_{mP}/P_{rP} \cong 7$. On the other hand, one cannot say whether insertion into the Mt–$CH_2CH(CH_3)$–$^{13}CH_3$ bond (first propagation step) is stereospecific or not. From the relative areas of the resonances of the enriched methylenes of sample 2 ([$\delta t\zeta t$]:[$\delta e\zeta e$]:[$\delta t\zeta e$]:[$\delta e\zeta t$] = 1.0:0.4:0.2:0.05) and considering the insertion steps leading to these end groups, it may be seen that insertion

0024-9297/86/2219-2703$01.50/0